

RESEARCH

Open Access



MASP1 in stomach adenocarcinoma: linking diagnosis, prognosis, and tumor immunity

Chuyu Xiao^{1,3}, Fuyang Hong^{1,2}, Guanzi Chen^{1,2}, Wenli Xu^{4*} and Yusheng Jie^{1,2,5*}

*Correspondence:

Wenli Xu

Xuwenli6@foxmail.com

Yusheng Jie

jieyush@mail.sysu.edu.cn

¹The Third Affiliated Hospital of Sun Yat-sen University, Guangzhou 510630, Guangdong, China

²Guangdong Provincial Key Laboratory of Liver Disease Research, Department of Infectious Diseases, The Third Affiliated Hospital of Sun Yat-sen University, Guangzhou 510630, Guangdong, China

³Department of Gastroenterology, The Third Affiliated Hospital of Sun Yat-sen University, Guangzhou 510630, Guangdong, China

⁴Division of Hepatobiliary Surgery, The First Affiliated Hospital of Guangxi Medical University, Nanning 530021, Guangxi, China

⁵Department of Infection, Lianzhou People's Hospital, Lianzhou 513400, Guangdong, China

Abstract

Background This study explored the role of Mannose-Binding Lectin-Associated Serine Protease 1 (MASP1) in the diagnosis, prognosis, and immune landscape of stomach adenocarcinoma (STAD), with the aim of providing a molecular foundation for developing early, non-invasive diagnostic tools and advancing immunotherapeutic strategies.

Methods We analyzed STAD messenger RNA (mRNA) data from The Cancer Genome Atlas (TCGA), immune-related gene data from the ImmPort database, and complement system-related genes from previous studies. Differentially expressed mRNAs (DEmRNAs) relevant to prognosis, immunity, and the complement system were identified using the “limma” and “survival” packages, alongside a Venn diagram. We confirmed MASP1 expression through analysis of external databases, as well as performing quantitative reverse transcription polymerase chain reaction (qRT-PCR) and Western blotting (WB) on the normal gastric cell line and various gastric cancer cell lines. The diagnostic performance of MASP1 was evaluated through Receiver Operating Characteristic (ROC) curve analysis using the “pROC” package. Chi-square tests were conducted to examine the association between MASP1 expression and clinicopathological factors. Univariate and multivariate Cox regression analyses were performed to quantify the survival impact of MASP1 expression. Enrichment analyses were conducted to elucidate the functions and pathways associated with MASP1. The relationship between MASP1 expression and tumor immune infiltration was analyzed using single-sample Gene Set Enrichment Analysis (ssGSEA), Cell-type Identification By Estimating Relative Subsets Of RNA Transcripts (CIBERSORT), Estimation of STromal and Immune cells in MAlignant Tumor tissues using Expression data (ESTIMATE), and Spearman correlation methods.

Result Our findings demonstrated that MASP1 is a significant biomarker associated with immune response and prognosis in STAD patients. Elevated MASP1 expression was correlated with poorer clinical outcomes, with ROC curve analysis revealing an Area Under the Curve (AUC) of 0.725 for MASP1. Additionally, MASP1 was identified as an independent prognostic marker for overall survival (OS) in STAD patients. The expression of MASP1 in STAD was predominantly linked to DNA damage repair and cell cycle regulation mechanisms. Furthermore, MASP1 expression showed a significant association with tumor-infiltrating immune cells and immune-related molecules.



Conclusion This study highlights the significant correlation between MASP1 and the immunological landscape of STAD. MASP1 has the potential to serve as a diagnostic and prognostic marker and could be a promising therapeutic target for immunotherapy in STAD.

Keywords MASP1, Stomach adenocarcinoma, Immune infiltration, Immune checkpoint

1 Introduction

STAD remains a significant global health concern due to its high incidence and mortality rates. Despite notable progress in diagnostic and therapeutic strategies, early detection of STAD remains challenging. The complexity of the disease is further compounded by the heterogeneity of cancer cells and the intricate dynamics of the tumor microenvironment (TME) [1]. The prognosis for STAD often suffers due to advanced stages at the time of detection. Research has now identified critical biomarkers that are revolutionizing treatment personalization. The human epidermal growth factor receptor 2 (HER2) - focused drug trastuzumab is at the forefront, with vascular endothelial growth factor (VEGF) and Claudin 18.2 also emerging as significant targets [2]. Therefore, conventional one-size-fits-all treatments are giving way to precision medicine, spurred by genetic insights that distinguish various STAD subtypes. The future of STAD therapy looks to leverage cutting-edge biotechnologies and tailored treatments including novel vaccines, targeted therapies, and immunotherapies. As biotechnological advancements accelerate, a shift towards individualized treatments for STAD, guided by detailed molecular and immune profiling, is expected to enhance survival rates and quality of care [3]. Hence, enhancing the early-phase detection rates of STAD, optimizing the efficacy of immunotherapy, and prolonging patient survival necessitate the identification of reliable biomarkers.

The innate immune system incorporates the complement system as a crucial detection and response mechanism that, upon activation, facilitates the removal of pathogens. Among its three activation pathways, the lectin pathway is integral, functioning through the attachment of mannan-binding lectin (MBL) or ficolin (FCN), which triggers the activation of MASPs including MASP1 and Mannose-Binding Lectin-Associated Serine Protease 2 (MASP2) [4]. Activated MASP1 cleaves Complement Component 3 (C3) into C3b and activates the alternative pathway under the participation of factor B and properdin [5–7]. Consequently, the lectin pathway, with the involvement of MASP1, along with the alternative pathway, is essential in the complement system. This results in the formation of the membrane attack complex (MAC), which orchestrates a range of biological functions, including cytotoxicity, opsonization, inflammation, and the clearance of circulating immune complexes (CICs) [8]. The role of complement system in cellular metabolism and intracellular signaling has opened new research avenues with therapeutic potential. Recent findings reveal its significant influence on the TME by modulating tumor growth, immune responses, and angiogenesis, impacting malignancy progression and treatment response. These insights have propelled the development of complement-targeted cancer immunotherapies, promising to refine and improve cancer treatment strategies [9]. Immunotherapeutic strategies that facilitate the cytotoxic action of T cells infiltrating both primary and metastatic tumors may benefit from targeting the complement system. This strategy may also play a critical role in overcoming immune exclusion

in tumors characterized by the absence of T cell infiltration. For instance, in a preclinical study targeting non-small cell lung cancer, researchers found that combining immunotherapies that inhibit both the Programmed Cell Death Protein 1 (PD-1) pathway and the complement protein C5a significantly reduced tumor growth and metastasis, while also prolonging survival in mouse models [10]. To date, there has been no literature documenting the mechanistic roles of MASP1 in STAD, nor its impact on patient prognosis or its association with immune cells infiltration within the tumor. Accordingly, this study utilizes comprehensive data analysis to investigate the expression of MASP1 in STAD, its association with patient prognosis, tumor-infiltrating immune cells, and immune-related molecules. The findings of this research aim to establish MASP1 as a potential biomarker for non-invasive diagnosis and to provide insights that could guide the development of innovative immunotherapeutic strategies for STAD.

2 Materials and methods

2.1 Collection of expressing data

Expression data were obtained from UCSC XENA (<https://xenabrowser.net/datapages/>), where RNAseq data in Transcripts Per Million (TPM) format from The Cancer Genome Atlas (TCGA) and Genotype-Tissue Expression (GTEx) were uniformly processed using the Toil pipeline. We extracted STAD-specific data from TCGA and normal tissue data from GTEx. Additionally, we acquired gene expression profiles from the Gene Expression Omnibus (GEO) database, specifically GSE19826, GSE79973, and GSE54129.

2.2 Identification and analysis of DE mRNAs

The “Limma” package was used to identify DE mRNAs with an absolute log₂ fold change greater than 1 and an adjusted P-value below 0.05. Subsequently, mRNAs co-expressed with the gene of interest were determined using R programming. For data visualization, the “ggplot2” package was employed to create a volcano plot of the identified mRNAs and a heatmap illustrating the relationship between MASP1 and its co-expressed mRNAs.

2.3 Prognostic analysis

The prognostic significance of MASP1 in STAD patients was evaluated using the “Survival” package. Patients were divided into high and low expression groups based on the median expression levels of the MASP1.

2.4 Identifying immune-related gene as prognostic marker

Immune-related genes were retrieved from the ImmPort database (<https://www.immport.org/shared/home>). Within the TME, the complement system plays a dual role. It can initiate cancer cell destruction but also facilitates tumor progression through anaphylatoxins that promote immunosuppression. This paradoxical function of the complement system underscores its potential as a target to enhance the efficacy of cancer immunotherapies [11]. Thus, a set of 53 complement system related genes was sourced from a prior research [12]. An intersection analysis, via a Venn diagram, was then conducted to elucidate the overlap between immune-related genes, prognostically significant DE mRNAs in STAD, and complement system related genes [12].

2.5 Analysis of MASP1 expression and ROC curves

MASP1 expression levels were analyzed using data from TCGA, accessed via the UCSC XENA platform. Expression patterns were visualized using the “ggplot2” library in R. To evaluate diagnostic potential, ROC curve analysis was conducted with the “pROC” package.

2.6 Survival analysis

We conducted proportional hazards assumption testing and fitted survival regression models using the “survival” package. For visualization of the results, we employed the “survminer” and “ggplot2” packages. When the optimal grouping method was applied, we used the “surv_cutpoint” function within the “survminer” package to determine the optimal cut-off point. The statistical method used was Cox proportional hazards regression, focusing on the gene MASP1. The analysis aimed to evaluate OS, progression free interval (PFI), and disease specific survival (DSS) as the prognostic measure.

2.7 Development and assessment of nomograms for predicting survival in STAD

In this study, we identified all significant clinicopathological prognostic factors using Cox regression analysis and developed a contingency table to assess the 1-, 3-, and 5-year OS probabilities for STAD patients. To validate the accuracy of the nomogram, we compared the predicted survival probabilities with the observed actual probabilities using a calibration curve. The alignment of the reference lines indicated that the model predictions were accurate.

2.8 Enrichment analysis

To elucidate the roles of MASP1, we implemented enrichment analyses via Gene Ontology (GO) and Kyoto Encyclopedia of Genes and Genomes (KEGG), alongside Gene Set Enrichment Analysis (GSEA). The “clusterProfiler” R package facilitated the automation of identifying GO terms and KEGG pathways. Stratification of STAD patients into groups with high and low MASP1 expression was based on the median expression level. To gain deeper insights into the gene’s function, GSEA was performed utilizing version 4.2.3 of the GSEA software.

2.9 Construction of protein-protein interaction (PPI) network

The construction of the PPI network utilized the Search Tool for the Retrieval of Interacting Genes (STRING) online database (version 12.0) [13], with parameters set as follows: network edge interpretation — confidence level, and minimum required interaction score — medium confidence (0.400) and subsequently, the generated PPI network was exported utilizing Cytoscape version 3.9.1.

2.10 Analysis of MASP1 within the context of immunity

We conducted a comprehensive correlation analysis to explore the relationship between MASP1, and a range of immune infiltration indices. The correlation coefficient was determined using Spearman’s rank correlation method due to its non-parametric nature, which makes no assumptions about the distribution of the variables in question. For the assessment of immune infiltration levels, we employed the ssGSEA algorithm, an approach incorporated within the R package “GSVA” (version 1.46.0). Visualization

of the resultant correlation data was achieved using the “ggplot2” package (version 3.3.6) for R (version 4.2.1). This was facilitated by crafting lollipop charts, which present a clear and effective graphical representation of the correlation strengths between MASP1 expression and the various infiltrating immune cells. Furthermore, evaluation of immune cell infiltration levels among STAD patients was performed by comparing groups with high versus low MASP1 expression, employing the Wilcoxon rank-sum test for statistical analysis.

2.11 Correlation analysis of MASP1 with immune related molecules

Immune checkpoints are critical modulators of the immune system, governing the fine balance between activation and inhibition to avoid unwarranted immune responses and ensure self-tolerance. These checkpoints, such as Cytotoxic T-Lymphocyte Antigen 4 (CTLA-4) and PD-1/Programmed Cell Death Ligand 1 (PD-L1) pathway, are key to preventing immune cells from indiscriminately attacking the body’s own tissues [14]. However, cancer cells can hijack these regulatory pathways to escape immune detection. To counter this, checkpoint inhibitors like ipilimumab [15], which targets CTLA-4, as well as pembrolizumab and nivolumab [16], which target PD-1, have been developed. These therapeutic antibodies disrupt the cancer-induced immune checkpoint engagement, reactivating the immune system against tumor cells and marking a transformative approach to cancer treatment. The Tumor and Immune System Interaction Database (TISIDB) serves as a comprehensive resource for analyzing the interactions between tumors and the immune system (<http://cis.hku.hk/TISIDB/>). To elucidate the immune-related role of MASP1 in cancer, we utilized the “Immunomodulator” module of the TISIDB to investigate the correlation between MASP1 expression and immune checkpoint gene levels. Furthermore, we explored the relationship between MASP1 and chemokine/chemokine receptor expression by assessing the expression levels of chemokines and their receptors in tumor-infiltrating immune cells using the “Chemokine” module.

2.12 Cell culture

The human gastric mucosal cell line GES1 was purchased from Applied Biological Materials and the STAD cell lines MKN28, MKN45 and MKN74 were gifted from Mingyue Zhang (Sun Yat-sen University Cancer Center, Guangzhou, China). Cells were cultured in Roswell Park Memorial Institute (RPMI) 1640 (abm Cat. No. TM503) containing 10% fetal bovine serum (FBS) (abm Cat. No. TM999) in a CO₂ incubator at 37 °C.

2.13 Western blot

GES1, MKN28, MKN45 and MKN74 cells were lysed with protease inhibitor and Radio Immunoprecipitation Assay (RIPA) lysis buffer for a 15-minute period on ice. Thereafter, this work adopted Pierce® BCA Protein Assay kit (Thermo Scientific, USA) in quantifying GES1, MKN28, MKN45 and MKN74 cellular proteins. For the detection of MASP1 protein, cellular proteins (30 µg) were separated on 10% tricine-Sodium dodecyl sulfate-polyacrylamide gel electrophoresis (SDS-PAGE), followed by electronic blotting on the 0.2-µM nitrocellulose (NC) membrane (Millipore). Later, western blot assay was conducted with anti-MASP1 (1:2,500, Proteintech, 21837-1-AP), anti-Glyceraldehyde-3-phosphate dehydrogenase (GAPDH) (1:5,000, Affinity Biosciences, #T0004). The Gel Imaging System (Syngene G: BOX F3, USA) was employed to observe signals.

2.14 RNA extraction and qRT-PCR

The total RNA was isolated from the cell lines using Trizol reagent (Invitrogen). cDNA was synthesized using a PrimeScript™ RT Reagent Kit with a gDNA Eraser Kit (Takara). PCR amplifications were constructed with the SYBR® Premix Ex Taq™ II (Takara) and normalized GAPDH for comparison. The $\Delta\Delta C_t$ method for the relative quantitation (RQ) of gene expression was used to determine GAPDH and MASP1 expression levels. The primer sequences used in this study are detailed as follows:

h-GAPDH-F: GGAGCGAGATCCCTCCAAAAT.

h-GAPDH-R: GGCTGTTGTCATACTTCTCATGG.

h-MASP1-F: GCTGGAGGCTCTCATACAGG.

h-MASP1-R: ACGTCCCATCCTTCAGACAC.

2.15 Statistical analysis

Utilizing IBM SPSS Statistics 25, we assessed the levels of MASP1 expression in both normal gastric and STAD tissue samples employing the Wilcoxon rank-sum and signed-rank tests. The relationship between MASP1 levels and various clinicopathological features was examined through the application of the chi-square test. To evaluate the prognostic impact of MASP1 expression alongside clinicopathological variables on patient survival, we conducted both univariate and multivariate Cox regression analyses, considering a P-value of less than 0.05 as indicative of statistical significance.

3 Results

3.1 Identification of MASP1 as the target gene

We identified 6650 DE mRNAs, which incorporates 4399 up-regulated mRNAs and 2251 down-regulated mRNAs between STAD tumor tissues and non-tumor tissues from TCGA and GTEx database. Immune-related genes were downloaded from the ImmPort database. We also obtained the complement system related genes from one previous study [12]. The Venn diagram was used to overlap the genes among immune-related genes, prognostic DE mRNAs in STAD and complement system related genes. The intersection identified two genes, MASP1 and Vitronectin (VTN) (Fig. 1a). Considering the molecule VTN yielded a modest AUC of 0.531 in the subsequent ROC analysis (Fig. 1b), it is deemed insufficient to warrant its inclusion as a target gene in our study. Therefore, MASP1, as the gene among the 2 overlapped genes which are prognostic DE mRNAs associated with immunity and complement system, was finally selected as the target gene. A volcano plot depicting the upregulated and downregulated genes in TCGA-STAD, with MASP1 clearly highlighted, was shown (Fig. 1c). The relationship between MASP1 and its co-expressed genes were illustrated by a heatmap (Fig. 1d), the first 5 genes (Phosphodiesterase 1 C (PDE1C), Klotho (KL), Tollid Like 1 (TLL1), Vesicle Amine Transport 1 Like (VAT1L), Growth Differentiation Factor 7 (GDF7)) that were positively correlated with MASP1 and the first 5 genes (Cyclin Dependent Kinase Regulatory Subunit 2 (CKS2), Ubiquinol-Cytochrome C Reductase Hinge Protein (UQCRH), Prothymosin Alpha (PTMA), GINS Complex Subunit 2 (GINS2), Cytochrome C Oxidase Subunit 5 A (COX5A)) that were negatively correlated with MASP1 were shown.

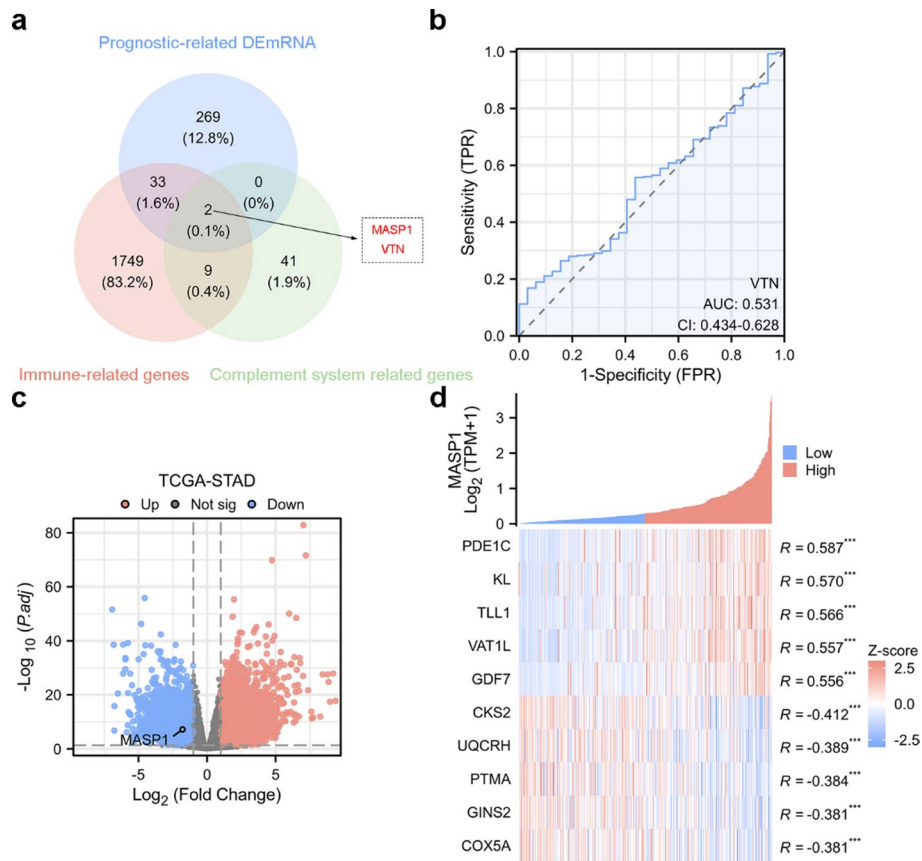


Fig. 1 Establishing MASP1 as the focus of this study. **a** Venn diagram highlighting the overlap among prognostic-related DE mRNAs in TCGA-STAD, immune-related genes, and complement system-associated genes, with MASP1 and VTN identified as intersecting candidates. **b** ROC curve analysis for VTN in TCGA-STAD. **c** Volcano plot showcasing differentially expressed genes in TCGA-STAD, with upregulated genes represented by red dots and downregulated genes by blue dots. The x-axis represents log-fold change (logFC), while the y-axis denotes $-\log_{10}(p\text{-adj})$. **d** Heatmap displaying MASP1 and its co-expressed mRNAs. ***, $P < 0.001$

3.2 A high level of MASP1 expression was strongly linked to poor prognosis in STAD

The expression of MASP1 in pan-cancer analysis from UCSC XENA database was shown (Fig. 2a). We can identify an expression decrease of MASP1 in tumor tissues compared with non-tumor tissues in STAD. The radar plot was also used to illustrate the MASP1 expression in tumor tissues compared with non-tumor tissues from a pan-cancer view (Supplementary Fig. S1a). The expression of MASP1 in STAD was visualized using data from the TCGA database. Tumor tissues exhibited significantly lower levels of MASP1 expression compared to non-tumor tissues in STAD (Fig. 2b, c). The AUC of the ROC curve was 0.725, indicating the potential role of diagnostic biomarker of MASP1 in STAD (Fig. 2d). According to the survival analysis, the OS was worse in MASP1 high group compared with MASP1 low group (Fig. 2e). Moreover, the DSS and PFI were also worse in MASP1 high group compared with MASP1 low group (Supplementary Fig. S1b, c). We then evaluated the prognostic impact of MASP1 across various cancer types and found that elevated MASP1 levels were associated with favorable prognosis in most cancers, including HNSC, KIRC, LGG, LIHC, and MESO, with the notable exception of STAD (Supplementary Fig. S1d). The distinct impact of MASP1 on the prognosis of STAD patients underscores a unique underlying mechanism specific to STAD.

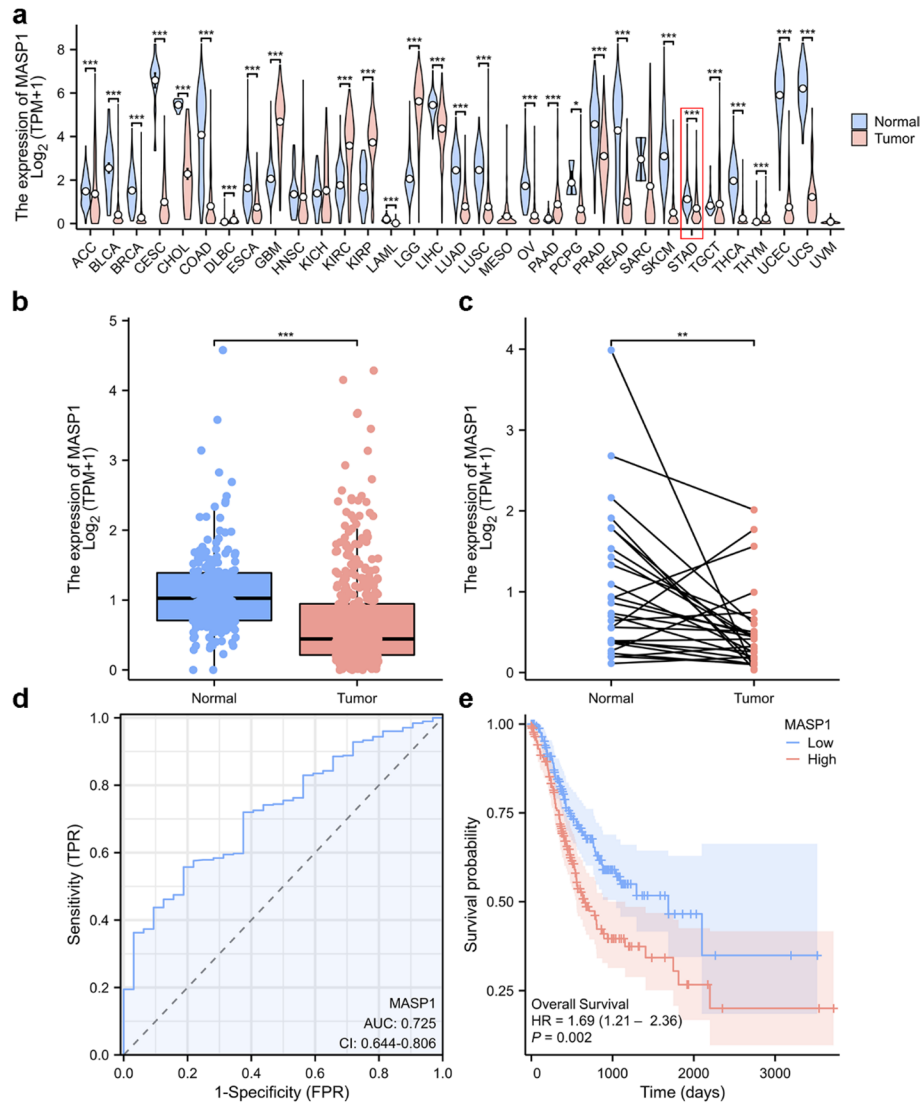


Fig. 2 Association of high MASP1 expression with poorer prognosis in STAD. **a** MASP1 expression across different types of cancer from the UCSC XENA database. **b, c** MASP1 expression in STAD based on data from the TCGA database. **d** ROC curve for MASP1 in TCGA-STAD. **e** Overall survival analysis of MASP1 expression from the TCGA dataset. *, $P < 0.05$, **, $P < 0.01$, ***, $P < 0.001$

3.3 Correlation between MASP1 expression and clinicopathological traits

The relationship between MASP1 expression and various clinicopathological traits were analyzed by a chi-square test (Table 1). Chi-square test illustrates that MASP1 was correlated to OS event (alive/dead) ($p < 0.01$) of STAD patients. MASP1 expression was slightly elevated in deceased STAD patients compared to those who were alive during the follow-up period (Fig. 3a). It was shown that the OS probabilities for patients in different STAD groups with high or low MASP1 expression. The results indicated that T4 subgroup of T stage ($p = 0.009$), N0 subgroup of N stage ($p = 0.046$), M0 subgroup of M stage ($p = 0.002$), without infection subgroup of H pylori infection ($p = 0.028$), and Stage III subgroup of pathological stage ($p = 0.025$) were associated with worse OS probability with elevated MASP1 expression (Fig. 3b-f).

To investigate the impact of MASP1 expression and clinicopathological characteristics on the survival of STAD patients, univariate and multivariate Cox regression analyses

Table 1 Association of MASP1 expression with clinicopathological characteristics (Chi-square test)

Characteristics	LOW expression of MASP1	High expression of MASP1	p-value
n	187	188	
Pathologic T stage, n (%)			0.737195253
T1&T2	47 (12.8%)	52 (14.2%)	
T3	84 (22.9%)	84 (22.9%)	
T4	53 (14.4%)	47 (12.8%)	
Pathologic N stage, n (%)			0.876176375
N0	58 (16.2%)	53 (14.8%)	
N1	46 (12.9%)	51 (14.3%)	
N2	38 (10.6%)	37 (10.4%)	
N3	35 (9.8%)	39 (10.9%)	
Pathologic M stage, n (%)			0.320516039
M0	164 (46.2%)	166 (46.8%)	
M1	15 (4.2%)	10 (2.8%)	
Pathologic stage, n (%)			0.951393271
Stage I	25 (7.1%)	28 (8%)	
Stage II	57 (16.2%)	54 (15.3%)	
Stage III	75 (21.3%)	75 (21.3%)	
Stage IV	20 (5.7%)	18 (5.1%)	
Primary therapy outcome, n (%)			0.831010856
PD	31 (9.8%)	34 (10.7%)	
SD	7 (2.2%)	10 (3.2%)	
PR	2 (0.6%)	2 (0.6%)	
CR	119 (37.5%)	112 (35.3%)	
Gender, n (%)			0.264378119
Female	72 (19.2%)	62 (16.5%)	
Male	115 (30.7%)	126 (33.6%)	
Age, n (%)			0.131102616
<= 65	75 (20.2%)	89 (24%)	
> 65	111 (29.9%)	96 (25.9%)	
H pylori infection, n (%)			0.210218252
No	74 (45.4%)	71 (43.6%)	
Yes	12 (7.4%)	6 (3.7%)	
Residual tumor, n (%)			0.825856364
R0	145 (44.1%)	153 (46.5%)	
R1	7 (2.1%)	8 (2.4%)	
R2	9 (2.7%)	7 (2.1%)	
Histologic grade, n (%)			0.302037427
G1	4 (1.1%)	6 (1.6%)	
G2	75 (20.5%)	62 (16.9%)	
G3	103 (28.1%)	116 (31.7%)	
Race, n (%)			0.84512056
Asian	38 (11.8%)	36 (11.1%)	
Black or African American	6 (1.9%)	5 (1.5%)	
White	115 (35.6%)	123 (38.1%)	
Histological type, n (%)			0.27176875
Diffuse Type	30 (8%)	33 (8.8%)	
Mucinous Type	5 (1.3%)	14 (3.7%)	
Not Otherwise Specified	107 (28.6%)	100 (26.7%)	
Papillary Type	3 (0.8%)	2 (0.5%)	
Signet Ring Type	4 (1.1%)	7 (1.9%)	
Tubular Type	38 (10.2%)	31 (8.3%)	
Anatomic neoplasm subdivision, n (%)			0.518551598
Antrum/Distal	73 (19.9%)	65 (17.7%)	

Table 1 (continued)

Characteristics	LOW expression of MASP1	High expression of MASP1	p-value
Cardia/Proximal	23 (6.3%)	25 (6.8%)	
Fundus/Body	66 (18%)	64 (17.4%)	
Gastroesophageal Junction	16 (4.4%)	25 (6.8%)	
Other	3 (0.8%)	1 (0.3%)	
Stomach (NOS)	2 (0.5%)	4 (1.1%)	
Antireflux treatment, n (%)			0.213545796
No	70 (39.1%)	72 (40.2%)	
Yes	14 (7.8%)	23 (12.8%)	
Reflux history, n (%)			0.50898401
No	91 (42.5%)	84 (39.3%)	
Yes	18 (8.4%)	21 (9.8%)	
Barretts esophagus, n (%)			0.75905705
No	98 (47.1%)	95 (45.7%)	
Yes	7 (3.4%)	8 (3.8%)	
OS event, n (%)			0.009242288
Alive	126 (33.6%)	102 (27.2%)	
Dead	61 (16.3%)	86 (22.9%)	
DSS event, n (%)			0.087967703
No	140 (39.5%)	123 (34.7%)	
Yes	39 (11%)	52 (14.7%)	
PFI event, n (%)			0.085438527
No	133 (35.5%)	118 (31.5%)	
Yes	54 (14.4%)	70 (18.7%)	

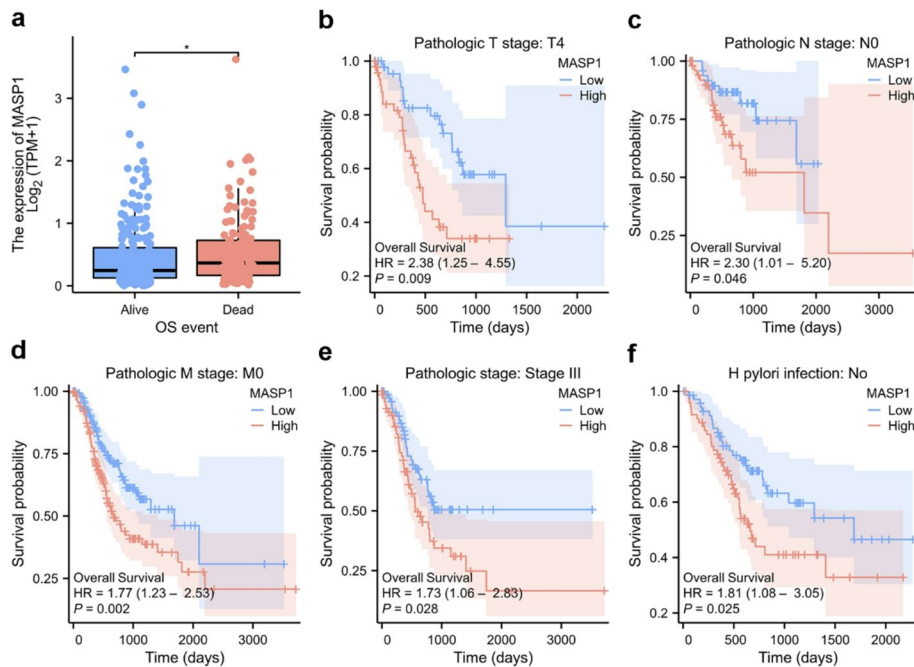


Fig. 3 Relationship between MASP1 expression and clinicopathological features. **a** MASP1 expression is associated with OS events in STAD patients. **b–f** Higher MASP1 expression in STAD subgroups was linked to worse overall survival. *, $P < 0.05$

were conducted. Variables with p less than 0.1 in the univariate analysis included age, T stage, N stage, M stage, pathological stage, primary therapy outcome, residual tumor, and MASP1 expression, all of which were found to be significant. Subsequently, a multivariate Cox regression model was developed, incorporating these variables alongside MASP1 expression. The analysis revealed that age ($p = 0.025$) and primary therapy outcome ($p < 0.001$) independently influenced the OS of STAD patients (Table 2). We also employed forest plots to present the outcomes of both univariate and multivariate Cox regression analyses (Supplementary Fig. S2a, b). We combined MASP1 expression levels with significant clinical variables identified in the univariate Cox regression analysis to create a nomogram for predicting patient survival probabilities at 1, 3, and 5 years. The nomogram illustrated that MASP1 expression provided superior prognostic accuracy compared to traditional clinical factors like age and sex (Fig. 4a). The accuracy of the nomogram was assessed by comparing predicted probabilities to observed actual outcomes using a calibration curve (Fig. 4b).

3.4 Verification of MASP1 expression using independent external databases and cell lines

Western blot analysis was performed to assess MASP1 expression in STAD cell lines. The results indicated that MASP1 expression was markedly reduced in MKN28, MKN45, and MKN74 cells compared to the normal gastric epithelial cell line GES1 (Fig. 5a). The

Table 2 Univariate and multivariate analysis of clinicopathological factors in STAD patients

Characteristics	Total(N)	HR(95% CI) Univariate analysis	P value Univariate analysis	HR(95% CI) Multivariate analysis	P value Multivariate analysis
Age	367				
<= 65	163	Reference		Reference	
> 65	204	1.620 (1.154 - 2.276)	0.005	1.936 (1.331 - 2.816)	< 0.001
Gender	370				
Female	133	Reference			
Male	237	1.267 (0.891 - 1.804)	0.188		
Pathologic T stage	362				
T1&T2	96	Reference		Reference	
T3&T4	266	1.719 (1.131 - 2.612)	0.011	1.224 (0.714 - 2.097)	0.463
Pathologic N stage	352				
N0&N1	204	Reference		Reference	
N2&N3	148	1.650 (1.182 - 2.302)	0.003	1.322 (0.832 - 2.099)	0.237
Pathologic M stage	352				
M0	327	Reference		Reference	
M1	25	2.254 (1.295 - 3.924)	0.004	2.472 (1.322 - 4.625)	0.005
Pathologic stage	347				
Stage I & Stage II	160	Reference		Reference	
Stage III & Stage IV	187	1.947 (1.358 - 2.793)	< 0.001	1.338 (0.754 - 2.373)	0.320
H pylori infection	162				
No	144	Reference			
Yes	18	0.650 (0.279 - 1.513)	0.317		
Histologic grade	361				
G1	10	Reference			
G2&G3	351	1.957 (0.484 - 7.910)	0.346		
MASP1	370				
Low	184	Reference		Reference	
High	186	1.688 (1.209 - 2.357)	0.002	1.838 (1.283 - 2.632)	< 0.001

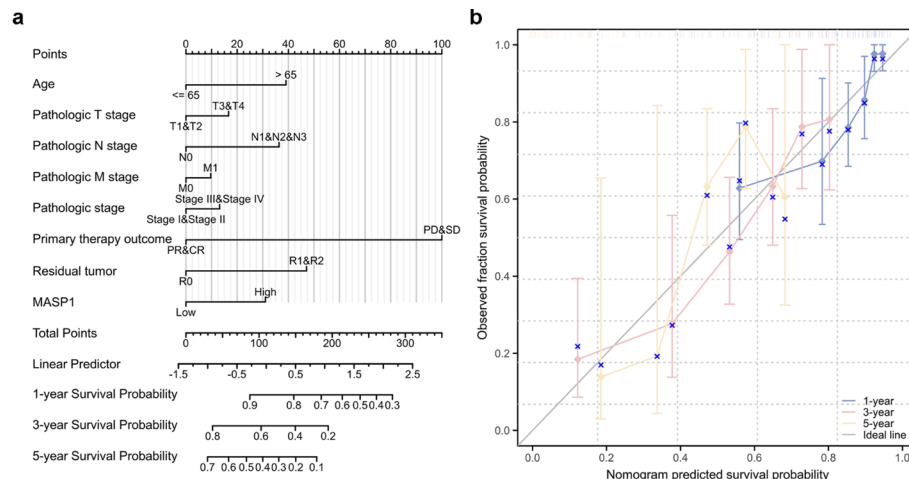


Fig. 4 Nomogram for predicting overall survival in STAD and its validation. **a** Nomogram for estimating 1-, 3-, and 5-year overall survival probabilities in STAD patients. **b** Calibration curve to assess the predictive accuracy of the nomogram

relative expression levels of MASP1 protein were also quantified (Fig. 5b). To further validate MASP1 expression levels in STAD, we analyzed three independent external GEO datasets (GSE19826, GSE54129, GSE79973) as a validation cohort. These datasets were used to compare MASP1 transcription levels between cancerous and adjacent noncancerous tissues. The analysis consistently demonstrated that MASP1 transcription levels were significantly lower in STAD tissues compared to adjacent normal tissues across all three datasets (Fig. 5c). qRT-PCR was employed to confirm the reduced MASP1 mRNA expression in MKN28, MKN45, and MKN74 cells compared to the normal gastric epithelial cell line GES1 (Fig. 5f).

3.5 Functional enrichment analysis and PPI

GO enrichment analysis is a bioinformatics technique used to identify over-represented GO categories within a gene set. This method highlights potentially significant biological processes (BP), molecular functions (MF), or cellular components (CC) that are systematically associated with specific conditions or treatments. By applying statistical tests, GO enrichment analysis determines whether certain GO terms appear more frequently than would be expected by random chance, thereby revealing underlying biological patterns in the dataset [17]. To clarify the biological processes and pathways associated with MASP1 in STAD, we conducted a series of analyses. Genes related to MASP1 (with a correlation coefficient greater than 0.4) identified through co-expression analysis were subjected to GO enrichment and KEGG pathway analyses. The primary GO and KEGG pathways that were significantly enriched are depicted (Fig. 6a, b). In STAD patients with high MASP1 expression, GSEA analysis indicated that the down-regulated hallmark gene sets were mainly enriched to pathways correlated to base excision repair, mismatch repair, homologous recombination and so on, the up-regulated hallmark gene sets were mainly enriched to pathways correlated to cell cycle (Fig. 7a-f). These findings suggest potential mechanisms through which elevated MASP1 contributes to disease progression, partially explaining the poor prognosis observed in STAD patients with high MASP1 levels. To pinpoint genes with regulatory patterns akin to MASP1 in STAD patients, we cross-referenced the top 708 genes most correlated with MASP1 and the

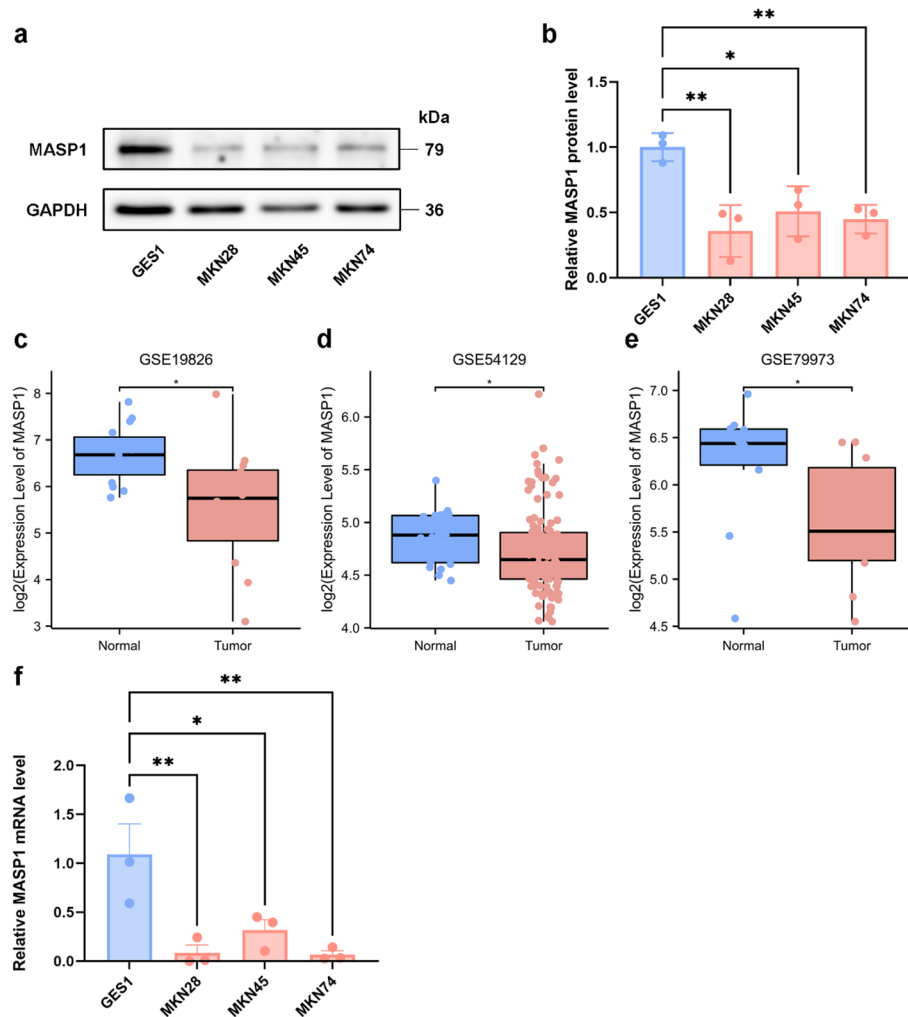


Fig. 5 Validation of the decreased MASP1 expression in STAD using independent cell lines and external datasets. **a** Western blot analysis of MASP1 protein levels in the normal human gastric epithelial cell line GES1 and various STAD cell lines, including MKN28, MKN45, and MKN74. **b** Quantification of relative MASP1 protein expression levels. **c-e** MASP1 expression in tumor and unmatched non-tumor tissues from the GSE19826, GSE54129, and GSE79973 datasets in the GEO database. **f** Quantification of relative MASP1 mRNA expression. *, $P < 0.05$, **, $P < 0.01$

346 survival-related downregulated genes in STAD, resulting in the identification of 130 intersecting genes associated with both MASP1 and STAD survival (Fig. 8a). We generated a heatmap for these 130 intersecting genes, revealing that they exhibit expression patterns similar to MASP1 (Fig. 8b). These 130 protein-coding genes have the potential to serve as genetic biomarkers for STAD patients. GO functional enrichment and KEGG pathway analyses, incorporating logFC data, were conducted on these genes. The top 5 enriched biological processes are regulation of microtubule-based process, mitotic sister chromatid segregation, chromosome segregation, vascular process in circulatory system and regulation of microtubule cytoskeleton organization (Fig. 8c); the top 5 enriched molecular functions are microtubule, condensed chromosome, centromeric region, spindle, chromosome, centromeric region and kinetochore (Fig. 8d); the 2 enriched cell components are tubulin binding and microtubule binding (Fig. 8e); the 5 enriched KEGG pathways are cGMP-PKG signaling pathway, Adrenergic signaling in cardiomyocytes, Salivary secretion, Aldosterone synthesis and secretion, and Oxytocin signaling

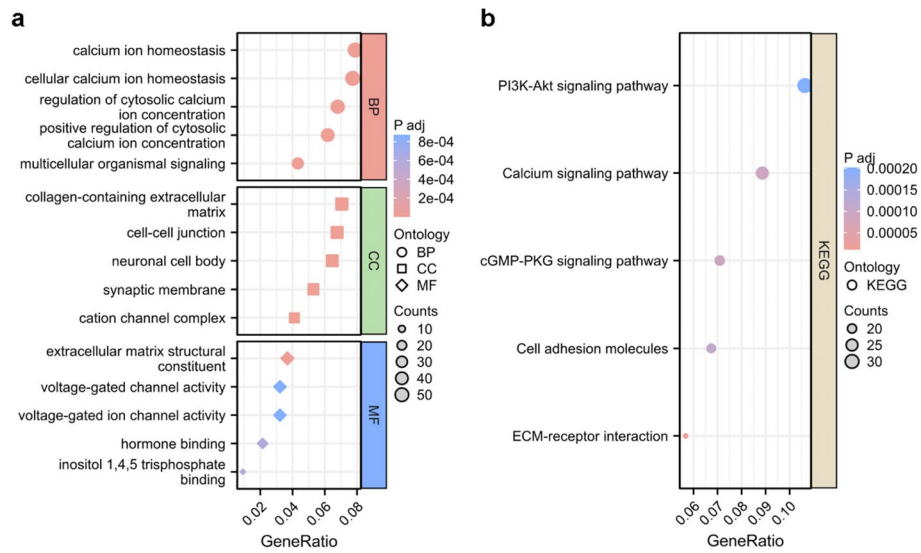


Fig. 6 GO and KEGG functional enrichment analysis of MASP1 in STAD. **a** The top 15 GO terms associated with MASP1 and its co-expressed genes. **b** The top 5 KEGG pathways related to MASP1 and its co-expressed genes

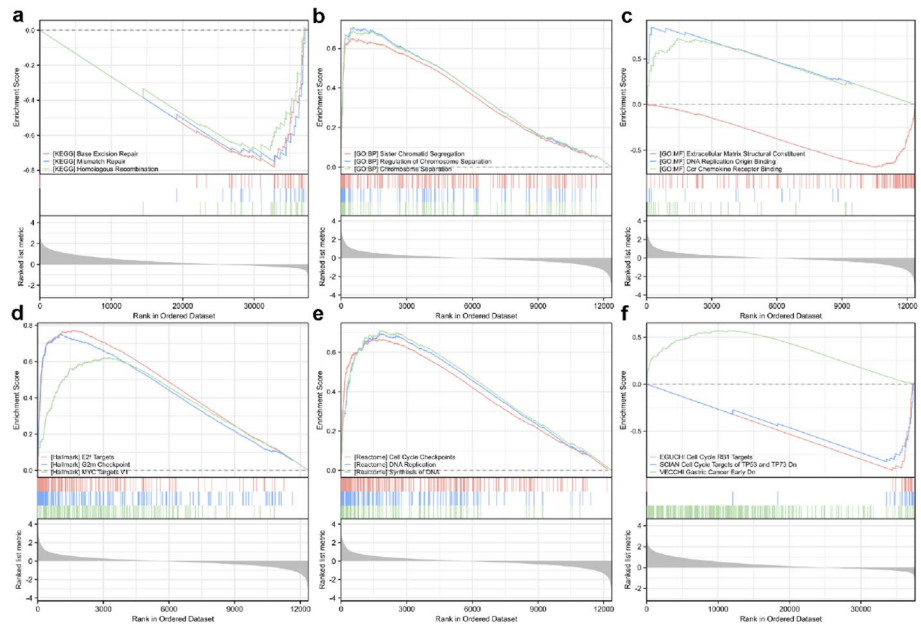


Fig. 7 GSEA. **a-f** Signaling pathways significantly enriched in STAD patients with elevated MASP1 expression

pathway (Fig. 8f). After identifying significantly different pathways, we conducted PPI and correlation analyses to examine the interactions among the 130 proteins. Our findings revealed a more robust enrichment network among these proteins compared to random protein interactions (Fig. 9a). Gene co-expression correlation analysis demonstrated that the majority of proteins within the network showed strong positive correlations with each other (Fig. 9b). Consequently, these MASP1-associated genes have the potential to act as multigene biomarkers for predicting the survival outcomes of STAD patients.

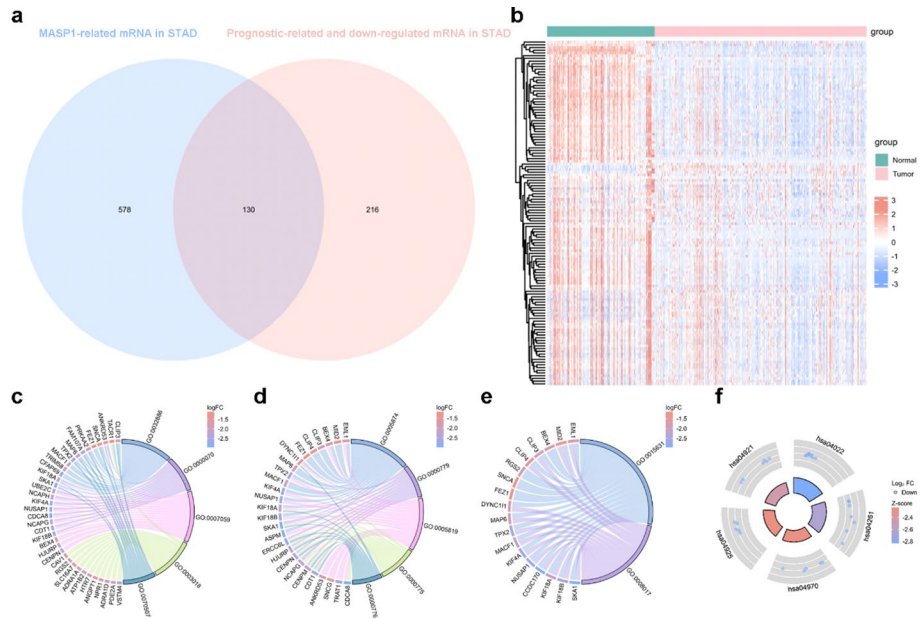


Fig. 8 MASP1 functional clustering and interaction network analysis of MASP1-related genes. **a** Venn diagram illustrating the overlap between MASP1-related genes in STAD and prognostic downregulated mRNAs in STAD. **b** Heatmap depicting the 130 intersected genes in TCGA-STAD. **c-e** Chord plot visualizing GO enrichment analysis of the 130 genes based on their LogFC. **f** Circle plot visualizing KEGG enrichment analysis of the 130 genes based on their LogFC

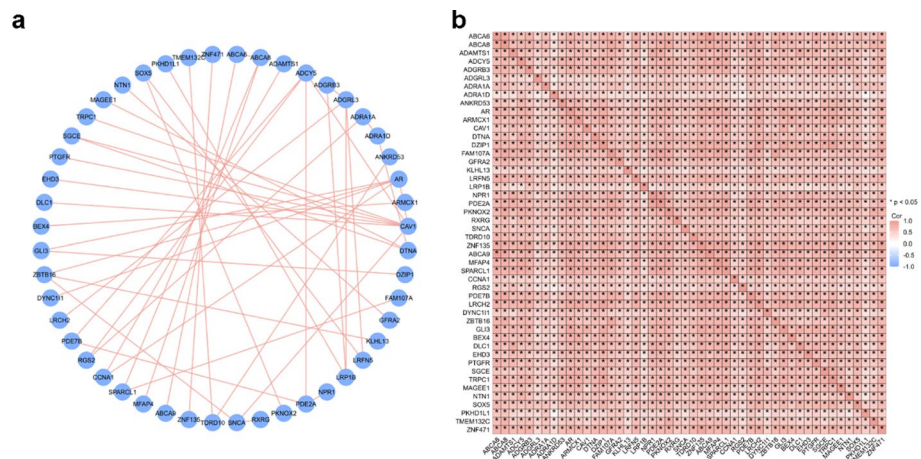


Fig. 9 MASP1-related gene interaction network (**a**) and gene co-expression matrix (**b**)

3.6 Correlation of MASP1 with tumor immunity

In this study, we noted that MASP1 expression is markedly reduced in STAD, indicating its potential involvement in the regulation of tumor immune responses. To further elucidate the relationship between MASP1 expression and tumor immunity, we analyzed immune cell infiltration in STAD specimens with varying levels of MASP1 expression. It was illustrated the associations between MASP1 expression and the relative abundance of 24 immune cell types in STAD, as determined using the ssGSEA algorithm (Fig. 10a). Various types of immune cells were demonstrated to be correlated with MASP1 expression, including Mast cells ($p < 0.001$, $r = 0.366$), plasmacytoid dendritic cells (pDCs) ($p < 0.001$, $r = 0.360$), effector memory T (Tem) cells ($p < 0.001$, $r = 0.343$), natural killer (NK)

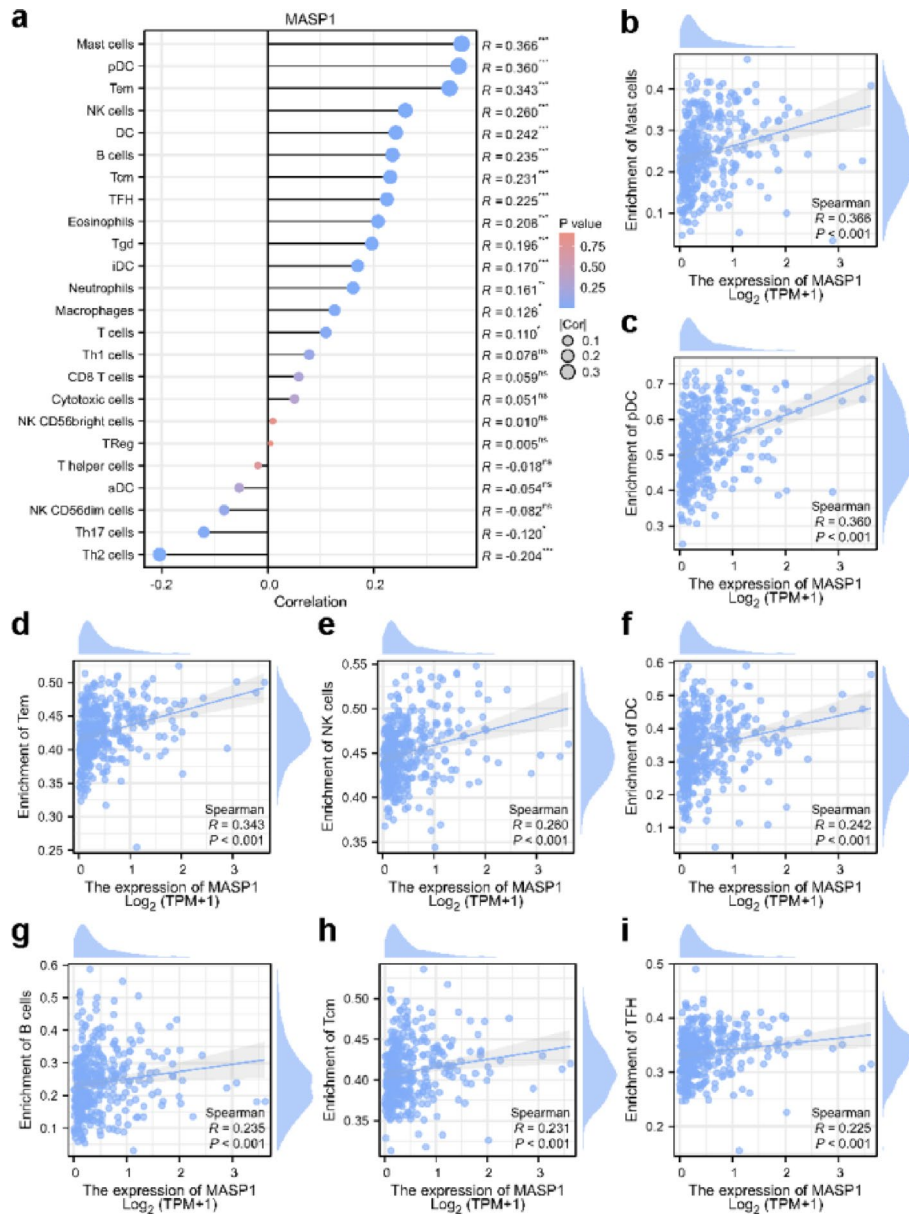


Fig. 10 MASP1 expression and tumor immunity. **a** Bar graph showing the correlation between MASP1 expression and 24 types of immune infiltrating cells. The x-axis represents the strength of the correlation, and the y-axis indicates the different immune cell types. MASP1 expression was positively correlated with **b** Mast cells, **c** pDCs, **d** Tem cells, **e** NK cells, **f** DCs, **g** B cells, **h** Tcm cells, and **i** TFH cells

cells ($p < 0.001$, $r = 0.260$), dendritic cells (DCs) ($p < 0.001$, $r = 0.242$), B lymphocytes (B cells) ($p < 0.001$, $r = 0.235$), central memory T (Tcm) cells ($p < 0.001$, $r = 0.231$), and follicular helper T (TFH) cells ($p < 0.01$, $r = 0.225$) (Fig. 10b-i). We further examined the correlations between MASP1 and immune cells from a pan-cancer perspective. The heatmap analysis revealed a strong association between MASP1 and tumor immunity across various cancer types (Supplementary Fig. S3a). We employed the CIBERSORT algorithm to analyze immune cell infiltration and observed consistent results (Supplementary Fig. S3b). The ESTIMATE algorithm was utilized to assess stromal and immune cell infiltration. The analysis revealed a correlation coefficient of 0.311 between MASP1 expression and the StromalScore (Supplementary Fig. S3c). Wilcoxon Rank-sum test was

utilized to discover the enrichment of immune cells in MASP1 high and low groups. The enrichment of all immune cells with significance were illustrated (Fig. 11a). Our results demonstrated that, compared with the MASP1 low expression group, the enrichment of Eosinophils, Mast cells, DCs, pDCs, B cells, Tcm cells, TFH cells, NK cells, immature dendritic cells (iDCs), Neutrophils, and Macrophages were higher in MASP1 high expression group (Fig. 11b-j). We also utilized stacked bar charts to visualize immune cell infiltration across high and low MASP1 expression groups. In these charts, different

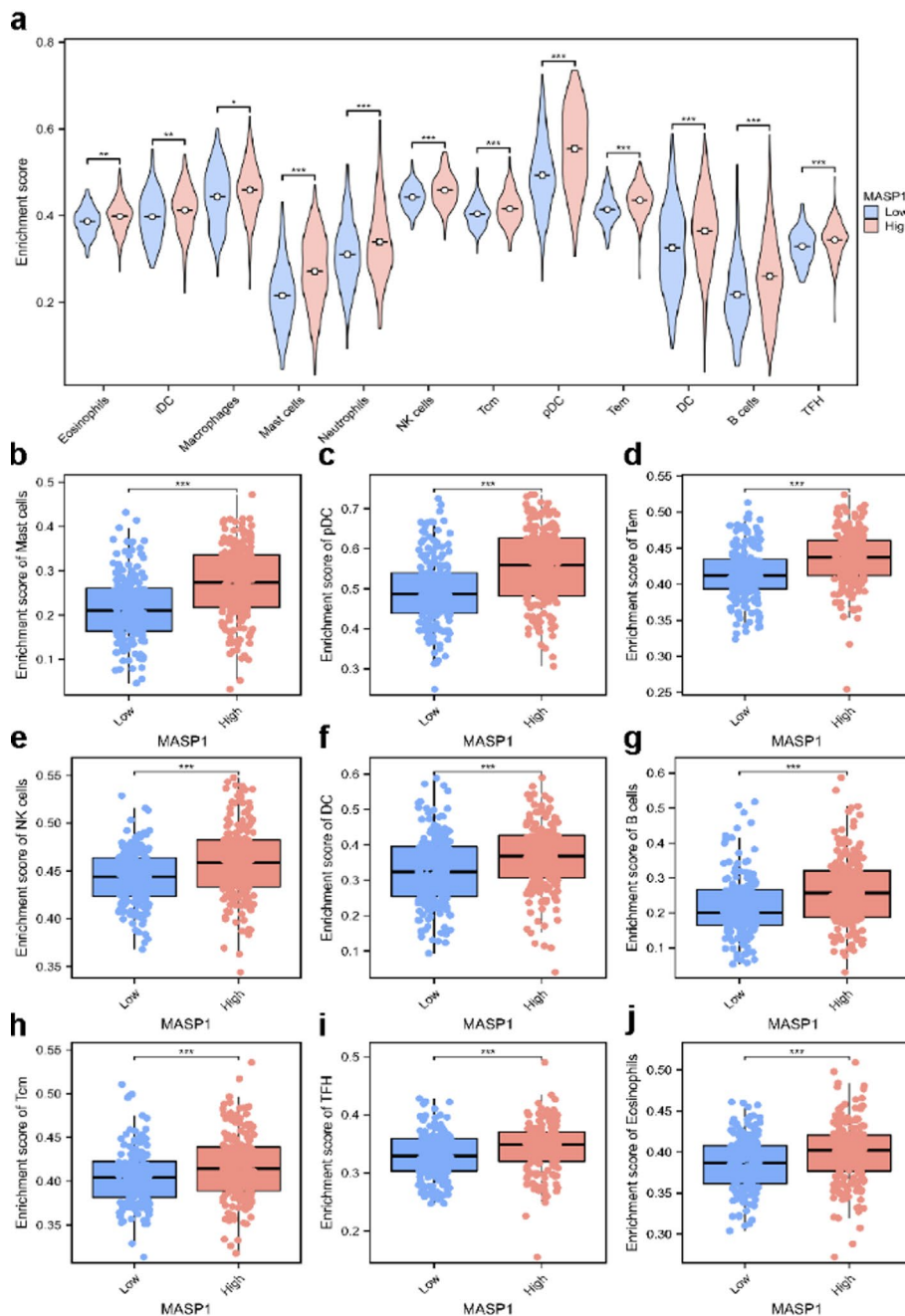


Fig. 11 The correlation between MASP1 expression and immune cell infiltration. **a** Immune cell infiltration in the MASP1 high and low expression groups. Compared to the low MASP1 expression group, the MASP1 high expression group in STAD showed higher levels of **b** Mast cells, **c** pDCs, **d** Tem cells, **e** NK cells, **f** DCs, **g** B cells, **h** Tcm cells, **i** TFH cells, and **j** Eosinophils. *, $P < 0.05$, **, $P < 0.01$, ***, $P < 0.001$

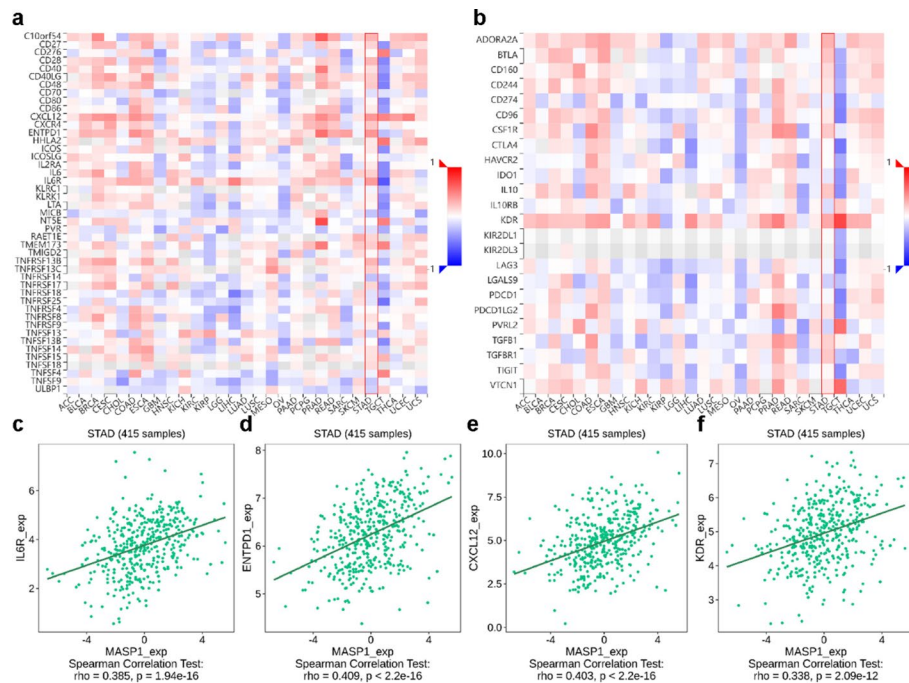


Fig. 13 Correlation analysis of MASP1 expression with immunostimulators and immunoinhibitors. **a** Heatmap showing the correlation between MASP1 expression and immunostimulators in tumors. **b** Heatmap illustrating the correlation between MASP1 expression and immunoinhibitors in tumors. **c–f** MASP1 expression is positively correlated with the immunostimulators IL6R, ENTPD1, and CXCL12, as well as with the immunoinhibitor KDR in STAD

receptors ($-0.3 < r < 0.3$). These findings suggest that MASP1 is positively correlated with specific chemokines/chemokine receptors in STAD.

Immune checkpoint inhibitors (ICIs) represent a groundbreaking approach in tumor immunotherapy, significantly enhancing the prognosis of patients with various cancer types [19]. We subsequently employed the TISIDB database to investigate the relationship between MASP1 expression and the levels of immunoinhibitors and immunostimulators across various human cancers (Fig. 13a, b). The results showed that the expression of MASP1 was positively correlated with Interleukin-6 Receptor (IL6R) ($r = 0.385$, $p < 1.94e - 16$), ectonucleoside triphosphate diphosphohydrolase 1 (ENTPD1) ($r = 0.409$, $p < 2.2e - 16$), CXCL12 ($r = 0.403$, $p < 2.2e - 16$), Kinase insert domain receptor (KDR) ($r = 0.338$, $p < 2.09e - 12$) (Fig. 13c-f). Thus, these findings indicate that MASP1 may potentially modulate tumor immunity.

4 Discussion

In the lectin pathway of the complement system, MASP1 is pivotal for activating MASP2, which then generates the C3 convertase by cleaving complement components C4 and C2. This cascade prompts both pathogen opsonization and initiation of the membrane attack complex. Additionally, MASP1 extends its functional repertoire by modulating coagulation and fibrinolysis, underlining its role beyond mere complement activation [20]. MASP1, traditionally associated with the lectin pathway of complement activation, is emerging as a factor in cancer development and progression. The underlying roles of MASP1 in various tumors have been reported, including non-small cell lung cancer (NSCLC), haematologic malignancies, cervical cancer and so on [21–23].

Given the scarcity of studies focusing on the role of the MASP1 in cancer, we conducted a comprehensive bioinformatics analysis to explore its biological functions and uncover potential regulatory pathways in STAD. Within the scope of TCGA, clinical profiles and RNA sequencing data for patients with STAD were acquired, and immune-related gene datasets were sourced from the ImmPort database. Subsequently, DE-mRNAs in STAD were identified using bioinformatic techniques. Through subsequent analysis with Venn diagrams, MASP1 was discerned as the gene of interest. Given its crucial role in the complement system, the function of MASP1 in STAD has not been extensively explored in prior research. Our investigation revealed that MASP1 expression levels are reduced in STAD tumor tissue when juxtaposed with normal gastric tissue and non-neoplastic gastric tissue by leveraging data of GTEx and TCGA from the UCSC XENA. Elevated MASP1 expression was observed to correlate with poorer OS outcomes and prognostication in STAD, alongside demonstrating a significant diagnostic utility. Moreover, Cox regression analysis underscored MASP1 as an independent prognostic factor, indicating the potential of MASP1 to serve as a valuable biomarker for both the diagnosis and prognosis in STAD patient care.

We first performed GO and KEGG enrichment analysis for MASP1-related mRNAs. The top five enriched biological processes were: Regulation of microtubule-based processes, Mitotic sister chromatid segregation, Chromosome segregation, Vascular processes in the circulatory system, and Regulation of microtubule cytoskeleton organization. These findings indicate that MASP1-related genes are significantly involved in cellular processes critical for mitosis and vascular homeostasis, suggesting a role in cell division and blood vessel formation. The top five enriched cellular components were: Collagen-containing extracellular matrix, Cell-cell junction, Cation channel complex, Neuronal cell body, and Synaptic membrane. This suggests that MASP1-related genes are associated with structural components of the extracellular matrix and cell junctions, as well as ion channel complexes and neuronal structures, highlighting their involvement in cellular architecture and communication. The top five enriched molecular functions were: Extracellular matrix structural constituent, Hormone binding, Inositol 1,4,5-trisphosphate binding, Voltage-gated ion channel activity, and Voltage-gated channel activity. These results imply that MASP1-related genes are crucial for the structural integrity of the extracellular matrix and are involved in hormone binding and ion channel activities, which are important for cellular signaling and function. The top five enriched KEGG pathways were: ECM-receptor interaction, Calcium signaling pathway, cyclic GMP-dependent protein kinase (cGMP-PKG) signaling pathway, Cell adhesion molecules, Phosphoinositide 3-kinase-Akt (PI3K-Akt) signaling pathway. These pathways highlight the role of MASP1-related genes in extracellular matrix interactions, calcium and cGMP signaling, cell adhesion, and PI3K-Akt signaling, all of which are pivotal in cellular communication, growth, and response to stimuli. In summary, the functional enrichment analysis indicates that MASP1-related genes are crucially involved in key cellular processes such as mitosis, extracellular matrix organization, and ion channel function. Additionally, these genes are implicated in essential signaling pathways that govern cellular adhesion and growth. Subsequently, we conducted GO and KEGG enrichment analyses, incorporating logFC data for MASP1-related mRNAs that demonstrated consistent expression patterns and regulatory effects on prognosis. The results of the enrichment analysis highlighted several key biological processes, cellular

components, molecular functions, and pathways. The top five enriched biological processes were: Regulation of microtubule-based process, Mitotic sister chromatid segregation, Chromosome segregation, Vascular process in circulatory system, and Regulation of microtubule cytoskeleton organization. These processes indicate that MASP1-related genes play significant roles in cell division and stability, particularly through the regulation of microtubules and chromatid segregation, which are critical for maintaining genomic stability and proper cell function. Additionally, involvement in vascular processes suggests a role in angiogenesis and vascular homeostasis, important for tumor growth and metastasis [24]. The top five enriched cellular components were: Microtubule, Condensed chromosome, centromeric region, Spindle, Chromosome, centromeric region, and Kinetochore. These components are primarily involved in the structural integrity and organization of chromosomes during cell division. The presence of these components underscores the importance of MASP1-related genes in mitotic processes and chromosomal stability [25]. The significantly enriched molecular functions included: Tubulin binding and Microtubule binding. These functions highlight the interactions of MASP1-related genes with microtubules, which are essential for maintaining cell shape, intracellular transport, and chromosome segregation during mitosis [25]. The top five enriched KEGG pathways were: cGMP-PKG signaling pathway, Adrenergic signaling in cardiomyocytes, Salivary secretion, Aldosterone synthesis and secretion, and Oxytocin signaling pathway. These pathways suggest diverse roles for MASP1-related genes beyond cell division, including signaling mechanisms that regulate physiological processes. The GO and KEGG enrichment analyses of MASP1-related mRNAs highlight their critical roles in key biological processes and pathways associated with cell division, genomic stability, and vascular processes. The enrichment in microtubule and chromosomal components, along with their molecular functions related to tubulin and microtubule binding, emphasizes their importance in mitotic processes. Additionally, the involvement in signaling pathways suggests broader regulatory roles in various physiological functions.

The GSEA conducted on mRNA expression data from STAD patients, segmented into high and low MASP1 expression cohorts, revealed significant pathway expression discrepancies when the low MASP1 expression group is employed as the reference. In the context of high MASP1 expression, there is an observable suppression of pathways associated with base excision repair, mismatch repair, homologous recombination, this downregulation suggests that these cancer cells may possess a diminished capacity to effectively repair DNA damage, leading to an accumulation of genetic mutations and increased genomic instability, which are characteristic features of cancer progression. Consequently, this genomic instability could contribute to heightened tumor aggressiveness, facilitating rapid disease progression and metastasis. Moreover, the specific impairment of DNA repair mechanisms in high MASP1 expression groups highlights potential therapeutic vulnerabilities, suggesting that these tumors may be particularly amenable to treatments that exploit DNA repair deficiencies, such as Poly (ADP-ribose) Polymerase (PARP) inhibitors [26]. Concurrently, the upregulation of pathways like sister chromatid segregation, regulation of chromosome separation, and chromosome separation. This heightened activity points to increased proliferative capacity, potentially driving tumor growth and aggressiveness. The findings imply that while these pathways may contribute to mitotic stability, they also represent a heightened oncogenic potential,

facilitating uncontrolled tumor expansion. Consequently, these upregulated pathways present potential therapeutic targets, as disrupting them could impede the aggressive proliferation characteristic of high MASP1 expression tumors [25]. Meanwhile, extracellular matrix structure constituent was downregulated in high MASP1 STAD patients, which could explain the poorer prognosis in high MASP1 group. These insights offer a deeper understanding of how MASP1 expression alterations in STAD may impact cellular pathways and functions, aiding in the elucidation of underlying mechanisms and potentially guiding the development of targeted therapeutic strategies.

In our study, the immune infiltration analysis revealed a notable positive correlation between the expression of MASP1 and the presence of various immune cell types within the tumor microenvironment of STAD patients. The cell types that showed this correlation include Mast cells, pDCs, Tem cells, NK cells, DCs, B cells, Tcm cells, TFH cells, eosinophils, gamma delta T (Tgd) cells, iDC and so on, suggesting the potential role of MASP1 in orchestrating a complex immune response within the tumor milieu, possibly by modulating complement system activation. This correlation encompasses an array of cells integral to both innate and adaptive immunity, hinting at MASP1's involvement in antigen presentation, cytotoxic activity, and perhaps the establishment of immunological memory—a facet that could prognosticate patient outcomes [27]. While these associations illuminate potential pathways for immunotherapeutic intervention, and position MASP1 as a prospective biomarker, they require robust experimental validation to confirm the mechanistic interplay between MASP1 expression and immune cell dynamics in the anti-tumor response. Moreover, the analysis indicated that the cohort with higher MASP1 expression levels showed a pronounced increase in an array of immune cells, such as Mast cells, pDCs, Tem cells, and B cells, when contrasted with the group presenting lower expression of MASP1. Our investigation into the association between MASP1 expression and established immune checkpoints such as PD-1, PD-L1, and CTLA-4 revealed no significant correlation. Further analysis extended to additional checkpoints like Lymphocyte-activation gene 3 (LAG3), B and T lymphocyte attenuator (BTLA), T cell immunoreceptor with Ig and ITIM domains (TIGIT), and V-set and immunoglobulin domain containing 4 (VSIR), where a positive correlation emerged between MASP1 expression and all but LAG3. In previous studies, Kin of Irregular Chiasm C-roughest Like (KIRREL) proteins were discovered to guide the wiring of sensory neurons in the mouse accessory olfactory bulb, impacting social and sexual behaviors. KIRREL3 ensures precise neuron cluster formation; its absence leads to fewer, larger clusters and reduced male aggression. KIRRELS act as a molecular code for neuron connections, crucial for both brain organization and behavioral responses [28]. Besides, KIRREL proteins in mice are key for organizing olfactory neuron axons into specific glomeruli by forming homodimers that guide axonal sorting. Disrupting KIRREL3's ability to dimerize impairs this organization, which is essential for proper olfactory function [29]. Recently, the role of KIRREL in various types of cancer has been reported. For example, Chen K et al. found elevated KIRREL levels in breast cancer correlate with unfavorable patient outcomes, suggesting its potential as a prognostic biomarker [30]. It was reported that the KIRREL expression in thin melanoma is linked with poorer outcomes and higher recurrence, indicating its potential as a prognostic marker for identifying high-risk patients in early disease stages [31]. Wang T et al. found KIRREL overexpression in gastric cancer boosted cell proliferation and angiogenesis via the

Phosphoinositide 3-Kinase/Protein Kinase B/Mechanistic Target of Rapamycin signaling (PI3K/AKT/mTOR) pathway, while its silencing impeded these processes. This relationship highlights KIRREL as a prospective target for anti-angiogenic cancer therapy [32, 33]. Therefore, our research assessed the relationship between MASP1 expression and the KIRREL protein family, specifically KIRREL1, KIRREL2, and KIRREL3. The findings demonstrated a notably strong positive association with the KIRREL protein family, most prominently with KIRREL1 and KIRREL3 (Supplementary Fig. S5a-c).

In conclusion, our analysis revealed that MASP1 expression is significantly reduced in STAD and is strongly associated with improved patient prognosis. MASP1 holds potential as a valuable marker for both the diagnosis and prognosis of STAD. Furthermore, MASP1 may influence STAD progression by modulating the cell cycle and immune infiltration, suggesting its potential as a novel prognostic biomarker for patients with STAD.

Supplementary Information

The online version contains supplementary material available at <https://doi.org/10.1007/s12672-025-02900-w>.

Supplementary material 1

Supplementary material 2

Acknowledgements

Not applicable.

Author contributions

Chuyu Xiao and Fuyang Hong conceptualized the study. Chuyu Xiao coordinated the study and oversaw data acquisition. Guanzi Chen and Fuyang Hong conducted experimental validation. Fuyang Hong and Chuyu Xiao performed the statistical analyses and interpreted the results. Chuyu Xiao and Guanzi Chen drafted the manuscript. Wenli Xu and Yusheng Jie provided overall project supervision, offering strategic guidance and contributing to the revision of the manuscript. All authors reviewed and approved the final manuscript.

Funding

This study have no funding.

Data availability

This research utilized RNA sequencing data and clinical information from the publicly available TCGA-STAD cohort. All bioinformatics tools and software applied in the analyses are openly accessible, and the manuscript provides comprehensive methodological details to ensure reproducibility.

Declarations

Competing interests

The authors declare no competing interests.

Ethical approval

Not applicable.

Consent to participate

Not applicable.

Consent for publication

Not applicable.

Received: 9 December 2024 / Accepted: 3 June 2025

Published online: 13 June 2025

References

1. Zavros Y, Merchant JL. The immune microenvironment in gastric adenocarcinoma. *Nat Rev Gastroenterol Hepatol*. 2022;19(7):451–67. <https://doi.org/10.1038/s41575-022-00591-0>.
2. Hogner A, Moehler M. Immunotherapy in gastric Cancer. *Curr Oncol*. 2022;29(3):1559–74. <https://doi.org/10.3390/currncol29030131>.
3. Hirata Y, Noorani A, Song S, Wang L, Ajani JA. Early stage gastric adenocarcinoma: clinical and molecular landscapes. *Nat Rev Clin Oncol*. 2023;20(7):453–69. <https://doi.org/10.1038/s41571-023-00767-w>.

4. Krarup A, Gulla KC, Gal P, Hajela K, Sim RB. The action of MBL-associated Serine protease 1 (MASP1) on factor XIII and fibrinogen. *Biochim Biophys Acta*. 2008;1784(9):1294–300. <https://doi.org/10.1016/j.bbapap.2008.03.020>.
5. Hajela K, Kojima M, Ambrus G, Wong KH, Moffatt BE, Ferluga J, et al. The biological functions of MBL-associated Serine proteases (MASPs). *Immunobiology*. 2002;205(4–5):467–75. <https://doi.org/10.1078/0171-2985-00147>.
6. Chen JY, Cortes C, Ferreira VP, Properdin. A multifaceted molecule involved in inflammation and diseases. *Mol Immunol*. 2018;102:58–72. <https://doi.org/10.1016/j.molimm.2018.05.018>.
7. Takahashi K, Banda NK, Holers VM, Van Cott EM. Complement component factor B has thrombin-like activity. *Biochem Biophys Res Commun*. 2021;552:17–22. <https://doi.org/10.1016/j.bbrc.2021.02.134>.
8. Conigliaro P, Triggianese P, Ballanti E, Perricone C, Perricone R, Chimenti MS. Complement, infection, and autoimmunity. *Curr Opin Rheumatol*. 2019;31(5):532–41. <https://doi.org/10.1097/BOR.0000000000000633>.
9. Kolev M, Markiewski MM. Targeting complement-mediated immunoregulation for cancer immunotherapy. *Semin Immunol*. 2018;37:85–97. <https://doi.org/10.1016/j.smim.2018.02.003>.
10. Ajona D, Ortiz-Espinosa S, Moreno H, Lozano T, Pajares MJ, Agorreta J, et al. A combined PD-1/CSa Blockade synergistically protects against lung Cancer growth and metastasis. *Cancer Discov*. 2017;7(7):694–703. <https://doi.org/10.1158/2159-8290.CD-16-1184>.
11. Magrini E, Minute L, Dambra M, Garlanda C. Complement activation in cancer: effects on tumor-associated myeloid cells and immunosuppression. *Semin Immunol*. 2022;60:101642. <https://doi.org/10.1016/j.smim.2022.101642>.
12. Gu X, Shen H, Zhu G, Li X, Zhang Y, Zhang R, et al. Prognostic model and tumor immune microenvironment analysis of Complement-Related genes in gastric Cancer. *J Inflamm Res*. 2023;16:4697–711. <https://doi.org/10.2147/JIR.S422903>.
13. Szklarczyk D, Kirsch R, Koutrouli M, Nastou K, Mehryary F, Hachilif R, et al. The STRING database in 2023: protein-protein association networks and functional enrichment analyses for any sequenced genome of interest. *Nucleic Acids Res*. 2023;51(D1):D638–46. <https://doi.org/10.1093/nar/gkac1000>.
14. Abril-Rodriguez G, Ribas A, SnapShot. Immune checkpoint inhibitors. *Cancer Cell*. 2017;31(6):848. <https://doi.org/10.1016/j.ccell.2017.05.010>.
15. Korman AJ, Garrett-Thomson SC, Lonberg N. The foundations of immune checkpoint Blockade and the ipilimumab approval decennial. *Nat Rev Drug Discov*. 2022;21(7):509–28. <https://doi.org/10.1038/s41573-021-00345-8>.
16. Malmberg R, Zietse M, Dumoulin DW, Hendriks J, Aerts J, van der Veldt AAM, et al. Alternative dosing strategies for immune checkpoint inhibitors to improve cost-effectiveness: a special focus on nivolumab and pembrolizumab. *Lancet Oncol*. 2022;23(12):e552–61. [https://doi.org/10.1016/S1470-2045\(22\)00554-X](https://doi.org/10.1016/S1470-2045(22)00554-X).
17. Vandenbrouck Y, Christiany D, Combes F, Loux V, Brun V. Bioinformatics tools and workflow to select blood biomarkers for early Cancer diagnosis: an application to pancreatic Cancer. *Proteomics*. 2019;19(21–22):e1800489. <https://doi.org/10.1002/pmic.201800489>.
18. Li J, Jie HB, Lei Y, Gildener-Leapman N, Trivedi S, Green T, et al. PD-1/SHP-2 inhibits Tc1/Th1 phenotypic responses and the activation of T cells in the tumor microenvironment. *Cancer Res*. 2015;75(3):508–18. <https://doi.org/10.1158/0008-5472.CA N-14-1215>.
19. Zhao X, Liu J, Ge S, Chen C, Li S, Wu X, et al. Saikosaponin A inhibits breast Cancer by regulating Th1/Th2 balance. *Front Pharmacol*. 2019;10:624. <https://doi.org/10.3389/fphar.2019.00624>.
20. Dobo J, Kocsis A, Gal P. Be on target: strategies of targeting alternative and lectin pathway components in Complement-Mediated diseases. *Front Immunol*. 2018;9:1851. <https://doi.org/10.3389/fimmu.2018.01851>.
21. Han S, Jiang D, Zhang F, Li K, Jiao K, Hu J, et al. A new immune signature for survival prediction and immune checkpoint molecules in non-small cell lung cancer. *Front Oncol*. 2023;13:1095313. <https://doi.org/10.3389/fonc.2023.1095313>.
22. Cedzynski M, Swierzko AS. Components of the lectin pathway of complement in haematologic malignancies. *Cancers (Basel)*. 2020. <https://doi.org/10.3390/cancers12071792>.
23. Maestri CA, Nishihara R, Mendes HW, Jensenius J, Thiel S, Messias-Reason I, et al. MASP-1 and MASP-2 serum levels are associated with worse prognostic in cervical Cancer progression. *Front Immunol*. 2018;9:2742. <https://doi.org/10.3389/fimmu.2018.02742>.
24. Nemeth Z, Debreczeni ML, Kajdacs E, Dobo J, Gal P, Cervenak L. Cooperation of complement MASP-1 with other proinflammatory factors to enhance the activation of endothelial cells. *Int J Mol Sci*. 2023. <https://doi.org/10.3390/ijms24119181>.
25. Maiato H, Gomes AM, Sousa F, Barisic M. Mechanisms of chromosome congression during mitosis. *Biology (Basel)*. 2017. <https://doi.org/10.3390/biology6010013>.
26. Yang X, Chen L, Mao Y, Hu Z, He M. Progressive and prognostic performance of an extracellular Matrix-Receptor interaction signature in gastric Cancer. *Dis Markers*. 2020;2020:8816070. <https://doi.org/10.1155/2020/8816070>.
27. Dobo J, Pal G, Cervenak L, Gal P. The emerging roles of mannose-binding lectin-associated Serine proteases (MASPs) in the lectin pathway of complement and beyond. *Immunol Rev*. 2016;274(1):98–111. <https://doi.org/10.1111/imr.12460>.
28. Prince JE, Brignall AC, Cutforth T, Shen K, Cloutier JF. Kirrel3 is required for the coalescence of vomeronasal sensory neuron axons into glomeruli and for male-male aggression. *Development*. 2013;140(11):2398–408. <https://doi.org/10.1242/dev.087262>.
29. Wang J, Vaddadi N, Pak JS, Park Y, Quilez S, Roman CA, et al. Molecular and structural basis of olfactory sensory neuron axon coalescence by Kirrel receptors. *Cell Rep*. 2021;37(5):109940. <https://doi.org/10.1016/j.celrep.2021.109940>.
30. Chen K, Zhao R, Yao G, Liu Z, Shi R, Geng J. Overexpression of kin of IRRE-Like protein 1 (KIRREL) as a prognostic biomarker for breast cancer. *Pathol Res Pract*. 2020;216(7):153000. <https://doi.org/10.1016/j.prp.2020.153000>.
31. Lundgren S, Fagerstrom-Vahman H, Zhang C, Ben-Dror L, Mardinoglu A, Uhlen M, et al. Discovery of KIRREL as a biomarker for prognostic stratification of patients with thin melanoma. *Biomark Res*. 2019;7:1. <https://doi.org/10.1186/s40364-018-0153-8>.
32. Zhang MJ, Hong YY, Li N. Overexpression of kin of IRRE-Like protein 1 (KIRREL) in gastric Cancer and its clinical prognostic significance. *Med Sci Monit*. 2018;24:2711–9. <https://doi.org/10.12659/MSM.910386>.
33. Wang T, Chen S, Wang Z, Li S, Fei X, Wang T, et al. KIRREL promotes the proliferation of gastric cancer cells and angiogenesis through the PI3K/AKT/mTOR pathway. *J Cell Mol Med*. 2024;28(1):e18020. <https://doi.org/10.1111/jcmm.18020>.

Publisher's note

Springer Nature remains neutral with regard to jurisdictional claims in published maps and institutional affiliations.